Analyst

Accepted Manuscript

ROYAL SOCIETY OF CHEMISTRY

www.rsc.org/analyst

Analyst

RSCPublishing

ARTICLE

Localized Surface Plasmon Resonance (LSPR) biosensing using gold nanotriangles: Detection of DNA hybridization events at room-temperature

Cite this: DOI: 10.1039/xoxxoooooox

Received ooth May 2014,
Accepted ooth 2014

DOI: 10.1039/xoxxoooooox

www.rsc.org/

Leonor Soares[a,b,c], Andrea Csáki[d], Jacqueline Jatschka[d], Wolfgang Fritzsche[d], Orfeu Flores[c], Ricardo Franco[a*], Eulália Pereira[b]

We present a proof-of-concept of the application of gold nanotriangles in sequence specific DNA detection, using localized surface plasmon resonance (LSPR) spectroscopy and dark field optical microscopy. The sensing platform comprises gold nanotriangles immobilized on a glass chip and oligonucleotides as probes. Probe formation and testing complementary and non-complementary targets followed common chip technology protocols. Gold nanotriangles showed remarkable sensitivity of 468 nm/RIU and allowed detection of 20mer targets. When this target sequence was part of a 50mer synthetic DNA oligonucleotide, LSPR shifts as high as 35 nm were observed. Conversely, when the target was present in PCR products of ca. 350 bp, obtained from clinical samples, LSPR shifts larger than 20 nm were observed. LSPR shifts were less than ± 1 nm for the respective non-complementary targets. These results with gold nanotriangles as sensors are a notable improvement to the LSPR shifts of less than 5 nm usually obtained for spherical gold nanoparticles of comparable sizes. Optimal conditions for detection of synthetic and PCR product targets with gold nanotriangles and oligonucleotides probes were achieved with low percentages of intercalating thioalkanes; target hybridization at room temperature; 3 hours of incubation; and 2x SSC buffer stringency conditions.

Introduction

Noble metal nanoparticles have been widely used as efficient probes for LSPR, due to their strongly enhanced surface plasmon resonance at optical frequencies, making them excellent scatterers and absorbers in the visible range. In addition to unique optical properties, gold nanoparticles (AuNPs) as binding platforms for biomolecules afford a stable immobilization of biomolecules, whilst retaining their bioactivities, which is a major advantage in biosensing applications.[1-4] Optical biosensors using AuNPs have shown to be exceptionally simple, fast, and reliable and have started recently to evolve from laboratory study to the point of practical use.[4, 5]. Nevertheless, there is still much room for improvement, and the next generation of biosensor platforms will require significant advances in sensitivity, specificity and parallelism in order to respond to future needs in a variety of fields ranging from medical diagnostics[6, 7] to environmental concerns related to the detection of hazardous substances.[8]

The localized surface plasmon resonance (LSPR) dependence of AuNPs on their dielectric environment is now being successfully used as a principle of detection of biological molecules.[9] Mechanisms of LSPR wavelength shifts are essentially based on analyte-surface binding interactions. These include the adsorption of proteins,[10] small molecules,[11] ligand-receptor binding,[12] protein adsorption on self-assembled monolayers,[13] DNA and RNA hybridization,[14-16] and protein-DNA interactions.[17] Analyte-binding interactions at the surface of the NP cause changes in the surface refractive index, which in turn is transduced into wavelength shifts of the LSPR extinction maximum. The versatile nature of LSPR for detection is also due to its strong dependence on nanoparticle composition, shape, size and interparticle spacing.[18]

Anisotropic nanoparticles present interesting physico-chemical properties, namely their shape and higher aspect ratios, leading to stronger dipole moments compared to spheres of similar size. These specific characteristics make the LSPR of anisotropic nanoparticles more sensitive to refractive index changes,[19] and increase the magnitude of induced fields. While a nanosphere exhibits dipolar resonance with degenerated longitudinal and transverse modes due to its spherical symmetry, increasing aspect ratio of an anisotropic nanoparticle leads to transverse and longitudinal modes splitting. From these two modes, three plasmon resonant peaks are observed at nanotriangles due to

anisotropy. Concurrently, the width of a LSPR peak typically increases as the sharpness of a tip or edge increases. This effect causes the dipolar fields of NP to be concentrated at these "hot spots", leading to enhanced electric fields, critical for surface enhanced spectroscopies.[20-22]

Triangular nanoparticles and LSPR have been applied to the development of a label-free detection method of PNA-DNA and DNA-DNA hybridization events.[23, 24] The binding and detection limits of the well know streptavidin-biotin system with silver nanotriangles[25] as probes, provided greater sensitivity when compared to SPR sensing techniques, due to the highly localized electromagnetic fields that occur at nanoparticle surfaces enabling improved detection of nanoscale biological analytes. Silver nanotriangles are widely used as biosensors in LSPR detection systems, and they have demonstrated a high rate of success in the field of DNA detection and even on gene mutation detection.[26] Silver has an advantage over other noble metals, as its LSPR energy is removed from inter band transitions (3.8 eV ~ 327 nm)[27] resulting in a narrow LSPR. In turn, this narrower band exhibits a much stronger shift upon increasing of the local dielectric constant as compared to the shift observed in AuNPs. On the other hand, silver NPs are more reactive than AuNPs, losing their original morphology and subsequently their sensitivity. Gold nanotriangles (AuNTs) are considerably more stable than their silver counterparts, maintaining their morphological characteristics throughout functionalization and conjugation processes, and for extended periods.[28]

One of the great challenges of modern molecular detection strategies is the integration of new genetic information into procedures that can be implemented in rapid, cost-effective and reliable methods. We and other groups developed an approach based on spherical AuNPs derivatized with thiol-modified oligonucleotides complementary to DNA targets.[29-32] The method has proven to be able to distinguish fully complementary from mismatched sequences.[31] Recently, an important advance was reached at the localized level, using gold nanospheres and DNA, combining dark field microscopy and LSPR spectroscopy.[16] It would then be highly desirable to use anisotropic AuNPs, namely AuNTs, to explore their new properties in terms of improved functionalization, bio-conjugation and detection sensitivity.

Here we propose a AuNTs-based biosensor for detection of DNA molecules that are complementary to a probe oligonucleotide ssDNA chain. This probe is attached to the surface of immobilized AuNTs. The post-treatment of the oligonucleotide-functionalized surface with a thioalkane, such as 6-mercaptohexanol (MCH), creating a mixed DNA/MCH monolayer, prevents nonspecific adsorption of the ssDNA chain to the AuNTs surface, while considerably improving hybridization events.[33] The sensing platform was tested for detection of both synthetic DNA targets and PCR-amplified targets obtained from clinical samples. Regarding the hybridization process, we investigated the influence of the position of a single mutation in the probe oligonucleotide sequence, on the efficiency of its hybridization to the target. With this purpose, a mismatched base was placed at the beginning (MUT5), at the middle (MUT10), or at the end (MUT20) of the thiolated probe.[15]

Experimental Section

Materials and methods

Sn (IV) meso-tetra(N-methyl-4-pyridyl)porphine tetratosylate chloride (SntMepyP) was from Frontier Scientific, Inc. (Logan, UT, USA). All other reagents were from Sigma-Aldrich or Carl Roth GmbH & Co. KG (Karlsruhe, Germany) and were of the highest purity available. Milli-Q water (18.2 Ω cm^{-1}) was used in the preparation of all solutions. All glassware was treated overnight with *aqua regia* (HNO_3 : HCl 1:3 v:v) and rinsed thoroughly with Milli-Q water before use. All the thiolated-oligonucleotides were purchased from STAB-Vida (Lisbon, Portugal) (Table 1-A) and the complementary/non-complementary synthetic targets DNA were from Eurofins MWG|Operon (Ebersberg, Germany) (Table 1-B):

Table 1 – A. Sequences of the thiolated oligonucleotides used for preparation of AuNT-probes. The poly-A spacer (italics) prevents steric hindrance upon target hybridization. The mutated base is indicated in bold; **B.** Sequences of synthetic targets used for the hybridization events. The complementary sequence is underlined.

A. Oligonucleotides (5'-HS to 3')	
noMUT	*AAAAAAAAAA*AGTTCCTTTGAGGCCAGGGA
MUT5	*AAAAAAAAAA*AGGG**C**CTACATTATCTTATC
MUT10	*AAAAAAAAAA*AGGCCAGGG**C**CTACATTATC
MUT20	*AAAAAAAAAA*AGTTCCTTTGAGGCCAGGG**C**

B. Targets (5' to 3')	
Complementary	TCAAGGAAACTCCGGTCCC**T**TTCCCATCAAGCC CTAGGGCTCCTCGTGGC'
Non-complementary	TTCCCATCAAGCCCTAGGGCTCCTCGTGGCTGCT GGGAGTTGTAGTCTGA

Synthesis and characterization of gold nanotriangles

The synthesis of AuNTs was performed using a previously developed photocatalytic method, with CTAB as the capping agent and a tin porphyrin, as photocatalyst.[34] UV-Vis spectra were obtained in a Varian Cary 50 Bio UV/Visible Spectrophotometer. Transmission Electron Microscopy (TEM) samples were prepared by casting 10 μL of AuNTs colloidal

solution into a carbon-coated copper grid 200 Mesh TAAB. TEM images were obtained with a HITACHI H-8100 electron microscope operated at 200 kV. Tapping mode scanning force microscopy (AFM) analysis of the sample was carried out using a NanoScope version 5.12, Dimension 3100.

Bulk refractive index sensitivity measurement

Water−glucose mixtures were used in order to determine the bulk refractive index sensitivity of the AuNTs. The concentration of glucose in the aqueous mixtures ranged from 0% (w/w) to 80% in steps of 10% resulting in a refractive index from n=1.333 to 1.420. A digital refractometer PAL-RI (Atago, Tokyo, Japan) was used to measure the refractive index of the glucose solutions, at controlled temperature (23 ºC).

Aliquots of 800 µL of CTAB-AuNTs colloidal solution were centrifuged (6 000 rpm, 10 minutes) in a Sigma UniCen DR15 centrifuge from Herolab GmbH, working with a 12024-H rotor. The pellet was resuspended in 1 mL of each glucose solution and the final solution incubated for 1 hour. Sensitivity was determined by plotting the LSPR wavelength of the longitudinal band as a function of the measured refractive index.

Gold nanotriangle deposition on glass chips

Sensor platforms were prepared from borosilicate glass chips with a microstructured chrome grating by deposition of AuNTs. Since it is necessary to compare the spectra of one particular nanotriangle before and after the consecutive steps of binding, the grating is essential to trace back individual AuNT after removal of the chips from the LSPR instrument for treatment. The grating was fabricated by a standard lift-off photolithographic process with a letter and a number in each grid. The tracking back is done by choosing an area near to the characters, which serves as a reference to identify the AuNTs in further steps (Figure S2).

Before use, each chip was washed by immersion in acetone, methanol, ethanol and water in ultrasonic bath for 10 minutes. After drying, the glass substrates were further cleaned by oxygen plasma etching (1 hour, 50 W, 5 Pa). The chips were functionalized with an amine surface group by treatment with 1% APTES (3-aminopropyltriethoxysilane) in 1 mM acetic acid for 10 minutes, followed by washing with water in an ultrasound bath for 5 minutes.[35] After drying, the chips were stored under argon atmosphere. Before AuNTs deposition, the chips were always re-activated by dipping in water in the ultrasound bath, for 10 minutes.

Before deposition of the AuNTs on the chips, the excess of CTAB and contaminating Au spheres in AuNT solution were removed by centrifugation (7 500 rpm, 10 minutes). The pellet was resuspended in 50 µL of water, and casted onto the glass surface. The chip was stirred for 1 hour in a platform mixer, at room temperature, then rinsed with water, and dried under a gentle nitrogen flow. The robustness of the deposition procedure was verified after each experimental step by checking for changes in the localization of individual nanotriangles in the chip. For all the experiments performed at 25 and 37 ºC no changes were detected, but desorption of the nanoparticles was detected at 59 ºC.

Oligo-functionalization of the immobilized AuNTs

Sensor platforms with immobilized AuNTs were immersed in a 1 µM solution of the oligonucleotide and incubated overnight in 1 M KH_2PO_4 buffer at room temperature. In order to increase hybridization efficiency[36, 37] the chips were dipped in 1 mM 6-mercaptohexanol (MCH) for 1 hour. Finally, the chips were dried under a gentle nitrogen flow, and used immediately after preparation.

Hybridization of the oligo-chips with synthetic targets

Solutions of 1 µM single-stranded synthetic DNA (ssDNA) targets were prepared in saline-sodium citrate buffer (SSC) at different concentrations (5x and 2x). Hybridization between the DNA targets and the probe immobilized at the surface of the AuNTs was performed by incubation of the oligo-chip with the target DNA solution for 3 hours at 25 ºC or at 37 ºC. Stringent washing of the chip was performed with 2 x SSC, followed by 0.2 x SSC, and finally water, in order to slowly decrease the ionic strength and remove unbound or non-specifically bound oligonucleotides. Finally, the chips were dried with a gentle nitrogen flow, and spectra of single particles were immediately obtained. DNA was extracted from saliva clinical samples in FTA Cards and PCR was performed, in order to amplify a 345 bp fragment from the human mini-chromosome maintenance 6 (MCM6) gene, using specific primers, and generating the complementary target. The MCM6 gene is located upstream from the lactase gene (LCT), and encodes for lactose phlorizin hydrolase (LPH). The choice of this specific fragment is due to its location, containing some of the polymorphisms related to lactose intolerance.[38] The non-complementary target was a FTO fragment of 455 bp showing no similarity with the probe, as confirmed using a basic local alignment search tool from BLAST.[39]. In order to obtain these fragments, two primers, namely two sequences previously designed were used (*FWR*: 5'-GAAGATGGGACGCTTGAATG-3' *REV*: 5'-CTGCGCTGGCAATACAGAT-3') together with Hot Taq DNA polymerase kit.

The purity of both PCR products was confirmed on 1.5% agarose gels before purification with ExoFAST-IT, a nuclease that eliminates unincorporated primers and dNTPs, according to the manufacturer's instructions (Figure S1), and quantification was performed by measuring $A_{260\ nm}$ (ε_{dsDNA} = 50 ng.cm/µL) using a NanoDrop 1000 spectrophotometer.

The temperature profiles – melting temperatures (T_m) - of the PCR products were obtained by high-resolution melting curve analysis using RotorGene 6500 (Corbett Research Pty Ltd, Sydney, Australia) and results were analyzed using the RotorGene 6000 series software, Version 1.7.65.

Hybridization of the oligo-chips with ssDNA from clinical samples

Since targets obtained from clinical samples are dsDNA (PCR products), it is necessary to obtain the corresponding ssDNA, before hybridization with the AuNT-probes. For this purpose, a 2x SSC solution with 1 μM of each PCR product was heated at 90 °C for 10 minutes in a thermo shaker, immediately followed by immersion in an ice bath for 10 minutes. The oligo-functionalized chip was then incubated in this previously denatured ssDNA solution at 20 °C for 3 hours. The chip was washed with 0.2x SSC and water, and finally dried under a nitrogen flow. The procedure was similar for both complementary and non-complementary targets.

Single particle micro-spectroscopy

Spectra of individual AuNTs were collected with an optical microscope Axio Imager Z1m (Carl Zeiss Micro-imaging, Göttingen, Germany) in dark field mode. A tungsten halogen lamp with a continuous spectrum and a color temperature of 3200 K serves as light source. A pinhole allowed for the collection of light from only a small (a few μm diameter) surface region, enabling single particle spectroscopy. Since the experiments were performed in dark field mode, the light collected through the pinhole is scattered light. The pinhole is coplanar to the tube lens, i.e. the pinhole is in the magnified, real image, and has a diameter of 150 μm. The light from the pinhole is passed through a multimode fiber to an Acton Research SpectraPro 2300i micro spectrometer (Princeton Instruments, Trenton, NJ, USA) with a grating with 150 lines per mm and a Peltier-cooled CCD camera.

For each experiment, single AuNTs were selected (Figure S2) and spectra obtained i) as deposited; ii) after functionalization with the oligonucleotide probes; and iii) after hybridization with either synthetic DNA targets, or DNA targets form clinical samples. Since the different steps may induce changes in the surface of the glass chip, a careful procedure for data analysis was used, as previously published.[16] In addition to the intensity of light scattered by the nanotriangles (I_{NP}) the contribution of background (I_{BG}), light source (I_{LS}) and dark current (I_{DC}) was also measured in each analysis. Data was corrected according to the following equation:

$$I = (I_{NP} - I_{BG}) / (I_{LS} - I_{DC})$$

All measurements were performed in air, and for each sample, ten to twelve nanoparticles were analyzed. Spectra were fitted with a Gaussian peak function using Origin 8.0 software, and were normalized to the peak intensity, in order to accurately determine the wavelength shift.

Results and discussion

Synthesis and characterization of gold nanotriangles

Gold nanotriangles were synthesized in high yield using a previously published photocatalytic method, which allows fine-tuning of the average size of the synthesized AuNTs34. The synthetic method uses CTAB, and the as-prepared AuNTs are designated as CTAB-AuNTs. The shape and size of the AuNTs were evaluated by TEM and AFM (Figure 1-A and 1-B, respectively) showing as expected that the samples contain mostly nanotriangles with side lengths in the range 80-100 nm (91 ± 17 nm) (Figure 1-C), with a few small spherical nanoparticles. The thickness of the nanotriangles as measured by AFM was ca. 17± 2 nm. The bulk extinction spectrum of CTAB-AuNTs (Figure 1-D) shows two bands: one that corresponds to the out-of-plane mode with a resonance at ca. 535 nm and that also has a significant contribution from non-triangular nanoparticles in solution, and another band corresponding to the in-plane mode, centered around 700-740 nm.[19]

An aspect that characterizes these specific AuNTs is the bulk RI sensitivity factor **S** (nm per refractive index unit (RIU)), a parameter that varies with the size, shape and material composition of the nanostructure. Regarding the characteristics mentioned above, measurements were performed by varying the refractive index (Δn) of the surrounding medium using aqueous solutions of glucose at different concentrations (0−80% glucose), implying a concomitant refraction index variation between $n_{0\%}$= 1.33 to $n_{80\%}$= 1.40. As refractive index values increase (measured with the refractometer), subsequent red-shifts are verified in the extinction spectra obtained from UV-Vis spectroscopy of the AuNTs for each sample. The resonance shift (Δλ) was calculated considering the maximum absorption wavelength for the first sample with 0% and the final sample with 80% glucose (Δλ= 34 nm). Considering the changes caused by the alteration of the refractive index of the solution, it is concluded that the AuNTs used in this study have a sensitivity factor of ~ 468 nm/RIU, which is in agreement with the range of values mentioned in the literature for equivalent silver nanotriangles coated with gold.

Optimization of the gold nanotriangle DNA detecting chip

In order to detect the specificity of DNA targets based on refractive index changes of AuNT-probes, special care was taken in the optimization of the sensing platform for LSPR measurements. Optimization involved nanoprobe preparation, namely optimal incubation times and solution conditions for AuNT-thiolated oligonucleotide functionalization and treatment with 6-mercaptohexanol (MCH), an alkanethiol that avoids non-specific DNA binding to the NP.

Gold nanotriangles capped with CTAB were immobilized on amine-modified glass chips, and 10-12 AuNTs with scatter peaks in the 650-700 nm range were selected for further analysis. Since the present method relies on the measurement of spectra from individual nanoparticles, it is in principle possible to select nanotriangles that show plasmon resonances in any desired range, but the use of a narrower range was found to be

unnecessary and time and labor consuming. On the other hand, we have also found that, in order to keep the resonance peak inside the wavelength range of the instrument used (350-900 nm), after functionalization and hybridization with DNA fragments, it is necessary to select nanotriangles with initial resonance peaks below the bulk average (ca. 750 nm). Spectra of the selected AuNTs were obtained after each surface modification step. Identification of individual AuNTs after each step was performed based on their position in the chrome grid of the glass slide (Figure S2). Under the LSPR microscope, CTAB-AuNTs can be identified as bright red dots, with LSPR spectra similar to the one presented in Figure 2 (dashed line). It is worth mentioning that in spite of all the modification steps, individual AuNTs could be detected in consistently the same positions on the grid. The LSPR spectra show a strong band corresponding to the in-plane mode. The out-of-plane dipole resonance and the quadrupole resonances are sometimes also detected as much lower intensity bands at lower wavelengths, as typically observed for silver and gold nanotriangles adsorbed to surfaces.[18-22] It should be mentioned that the symmetry of the resonance band is a strong indication that the spectrum is due to a single nanoparticle, and not to aggregates deposited on the chip.

The following modification step was AuNT functionalization with different thiolated oligonucleotides. All the oligonucleotides tested (see Table 1-A) contained a thiol group at the C-terminal, providing strong adsorption to the gold surface; a spacer of ten adenines (A) and a sequence of 20 nucleic bases complementary to the DNA target sequence. The adenine spacer is used to make the oligonucleotide more available for target hybridization, by moving the probe away from the AuNT surface. Preliminary AuNT functionalization experiments, performed with oligonucleotides without spacer, indicated that the hybridization step was clearly not as successful as in the presence of the adenine spacer (data not shown). A typical spectrum of oligo-modified nanotriangles is shown in Figure 2 (solid line).

For all the analyzed gold nanotriangles, a significant LSPR shift towards the red was observed ($\Delta\lambda_{max}$ = 15.2 ± 2.8 nm; Figure 2, compare dashed line with solid line) after incubation of the AuNTs with oligonucleotide noMUT for 15 hours. Such LSPR shift corresponds to a change of the immediate environment of the AuNTs from CTAB, a cationic surfactant, to DNA, which is related to a local refractive index change from n=1.435 (CTAB)[40] to n=1.462 (DNA).[41] As a control, a chip containing AuNTs was incubated in the same buffer conditions, but without probe oligonucleotide and the observed shift demonstrated to be ca. 30% ($\Delta\lambda_{max}$ = 4.1 ± 0.6 nm) of the observed LSPR shift in the presence of the thiolated oligonucleotide. This experiment and its control allow establishing a successful oligonucleotide functionalization of the immobilized AuNTs, forming AuNT-probes.

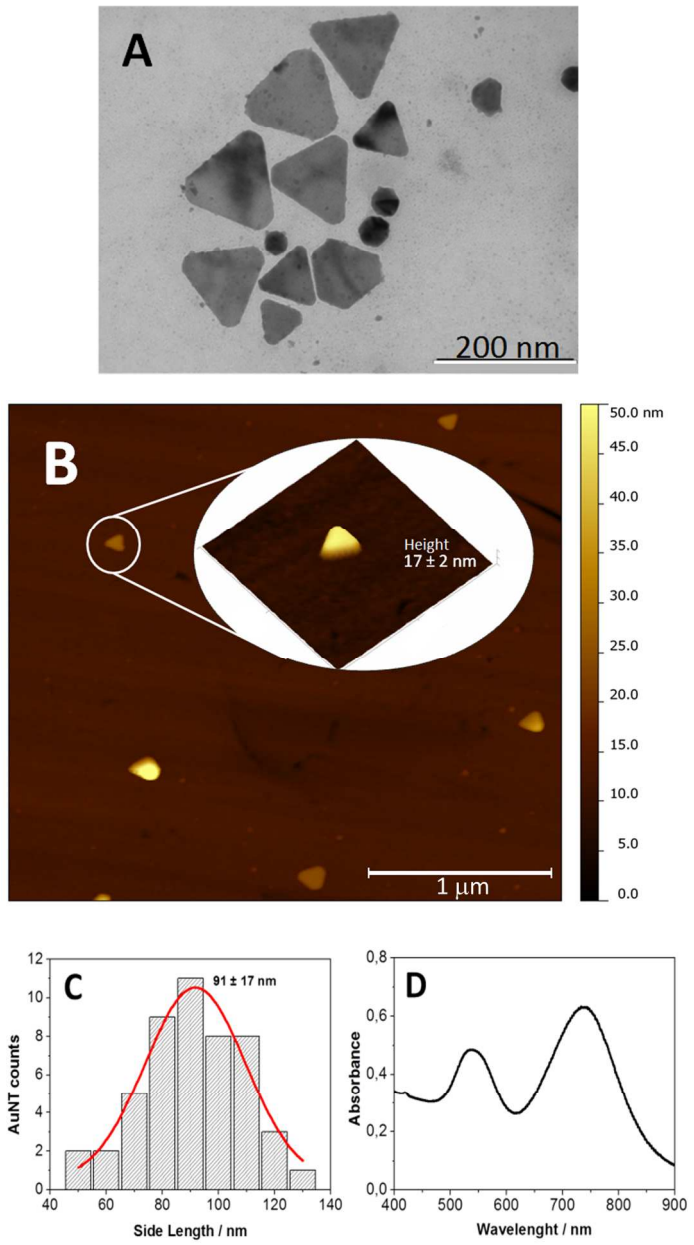

Figure 1: (A) Representative TEM image of CTAB-AuNTs. **(B)** Amplitude AFM picture of a selected area of the chip showing AuNTs (highlight of a single AuNT with 17 ± 2 nm thickness) **(C)** Histogram of distribution of side length; average side length: 91 ± 17 nm AuNTs (N=51 particles). **(D)** Visible extinction spectrum of a sample of CTAB-AuNTs in aqueous solution.

The incubation time of immobilized AuNTs with the oligonucleotide noMUT was also evaluated in order to obtain a sensitive and robust AuNT-probe. The LSPR signal shifted ca. 5 nm ($\Delta\lambda_{max}$ = 5.4 ± 1.1 nm) after 1 hour incubation of immobilized AuNTs with the oligonucleotide noMUT, and after 2 hours the LSPR shifted by $\Delta\lambda_{max}$ = 13.7 ± 3.6 nm. For longer incubation times, the increase in LSPR shift is much slower, until a $\Delta\lambda_{max}$ of 15.2 ± 2.8 nm for an incubation time of 15 hours. These results seem to indicate that after 2 hours, immobilized AuNTs are almost completely saturated with the

oligonucleotide.[33, 42] However, AuNT-probes prepared with 2 hours incubation prove to be unstable to the hybridization steps necessary for DNA detection (See section *Hybridization with DNA targets*). In fact, after hybridization with DNA targets the LSPR spectrum is similar to that of the initial CTAB-AuNTs. This is not the case for probes prepared with an incubation time of 15 hours with noMUT, which show a higher shift upon hybridization with the DNA target. Apparently, the binding of the oligonucleotide to the AuNTs, after an incubation of 2 hours is not strong enough to prevent detachment of the thiolated oligonucleotide from the AuNT surface upon hybridization with the DNA target and subsequent washing step. In contrast, after an incubation of 15 hours, oligonucleotide noMUT is strongly bound to the AuNT, and this detachment is no longer observed. This behavior can be explained assuming a two-step process for the binding of noMUT to the AuNTs. A first fast step in which the thiolated oligonucleotide adsorbs to the surface of the AuNTs. This first step would be driven mainly by electrostatic interaction between the positively charged surface (capped with CTAB, a positively charged surfactant), and the negatively charged oligo. The second step would be a slow rearrangement, during which the thiolated oligonucleotide binds through the thiol to the Au surface. Apparently, the electrostatic adsorption is not strong enough to endure the experimental conditions of the hybridization step, whereas thiol binding to the gold surface is sufficiently strong to prevent detachment of the oligonucleotide under the same experimental conditions.

In order to further optimize the preparation of the AuNT-probes, 6-mercaptoethanol (MCH) was used to form a mixed MCH/DNA monolayer. This type of mixed monolayers may promote hybridization with the DNA target by improving the accessibility of immobilized oligonucleotides to the complementary target sequences. The thiol group of MCH rapidly displaces the weaker adsorptive contacts between the oligonucleotide used as probe and the gold surface of the AuNT, leaving the probes tethered primarily through the thiol end groups.[43] Figure S3 summarizes optimization data for AuNT-probe formation with different thiolated oligonucleotides. Two different concentrations of MCH were tested, 1 mM and 5 mM. After incubation with oligonucleotides for 15 hours, the chips were dipped in MCH solution for 1 hour and the LSPR shift was measured. For 1 mM MCH a small LSPR shift was observed in relation to oligo-functionalized AuNTs (from $\Delta\lambda_{max}$ = 15.2 ± 2.8 nm, to $\Delta\lambda_{max}$ = 16.3 ± 3.1 nm), but for 5 mM MCH the LSPR shift was much higher ($\Delta\lambda_{max}$ = 23.8 ± 2.8 nm) than for AuNTs only with oligonucleotide noMUT. The red-shift upon MCH binding has been previously reported for gold nanospheres, and interpreted as evidence of the ability of MCH to intercalate between the thiol-oligonucleotide molecules yielding a more compact mixed monolayer around the nanoparticle[16]. This increases the amount of organic molecules around the nanoparticle, leading to the red-shift observed. For the gold nanotriangles the different shifts observed for the two concentrations used indicate that the extent of MCH binding to the nanoparticles is concentration-dependent in this concentration range, so both AuNT-probes (treated with 1 mM and 5 mM MCH) were used in the following target hybridization experiments in order to assess the effect of MCH binding on the sensor performance.

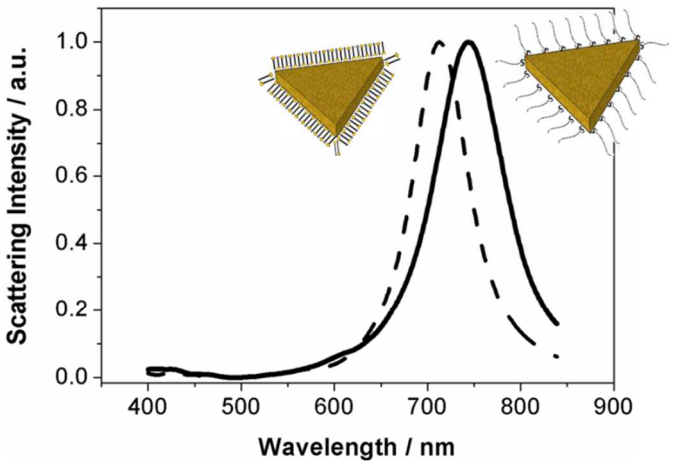

Figure 2: Representation of a typical spectrum of a selected AuNT (before and after functionalization); namely, from original CTAB capping (dashed line, maximum wavelength 697.2 nm) to oligonucleotide + MCH 1 mM (solid line, maximum wavelength 713.6 nm). Spectra were obtained after a 15 hours incubation period.

Hybridization with DNA targets

The basis of the proposed detection method for specific DNA sequences is the AuNT-probes plasmon resonance shift upon target DNA hybridization. It is expected for a DNA target that is complementary to the probe, *i.e.*, that specifically binds to the complete base sequence of interest, to contribute to an additional red-shift of the plasmon resonance, due to the increase of the amount of DNA at the AuNT surface. In contrast, if the target DNA is non-complementary, it will not hybridize to any part of oligonucleotide in the AuNT-probe, and the plasmon resonance does not change (Figure 3).

In order to optimize the DNA detection platform, different stringency conditions were tested for the hybridization process. For example, high stringency hybridization conditions such as high temperature and low salt buffers, allows only hybridization between base sequences that are highly similar.

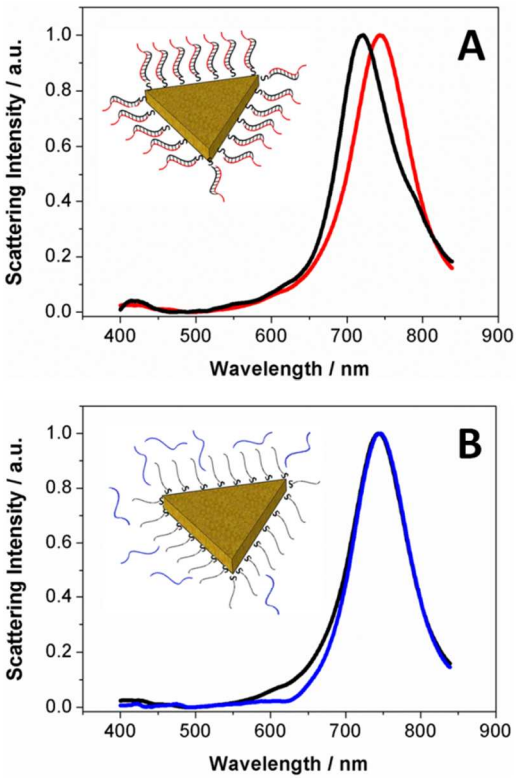

Figure 3: Schematic representation of the detection assay, namely, hybridization of the nanoprobe with a complementary **(A)** and non-complementary **(B)** target, and the corresponding LSPR spectra. Black traces correspond to LSPR spectra from the AuNT-probe before hybridization (maximum wavelength 713.6 nm); the red trace correspond to the LSPR spectrum after hybridization with the 1 μM complementary DNA target (maximum wavelength 748.7 nm) **(A);** and the blue trace corresponds to the LSPR spectrum in the presence of a 1 μM non-complementary DNA target (maximum wavelength 714.6 nm) **(B)**. Hybridization conditions were with 1 mM MCH and at 25 °C, using 2x SSC.

Synthetic targets

The experimental conditions were firstly optimized for synthetic targets in view of developing a proof-of-concept for using AuNT-probes for specific DNA sequence detection. These synthetic targets are ca. 7 times shorter (50 bp) than the PCR products obtained from clinical samples (ca. 350 bp). The synthetic targets were designed in order to contain a 20 bp sequence that totally matched the probe. Non-complementary targets used as negative control have total absence of complementarity to the probe used (Table 1-B). All synthetic targets used are single-stranded DNA (ssDNA) and it is thus possible to avoid the use of high temperatures necessary for DNA melting of the double stranded PCR products obtained from clinical samples.

In the optimization experiments for hybridization of synthetic targets with the AuNT-oligonucleotide noMUT probes the following conditions were studied: hybridization temperature (37 ºC and 25 ºC); incubation time (2-3 hours); SSC concentration (5x or 2x); and concentration of MCH used in the preparation of the AuNT-probes (1 mM and 5 mM, Table S1). The objective of these optimization experiments was to obtain the highest possible discrimination between the LSPR shifts after incubation of the AuNT-probes with the complementary target and with non-complementary target. For an incubation time of 2 hours at 37 ºC there is a significant red shift of the LSPR (24.3 ± 5 nm, 2x SSC; 20.3 ± 2.3 nm, 5x SSC, both for probes treated with 5 mM MCH), whereas an insignificant blue-shift of the LSPR is observed for the non-complementary target (Table S1). Although this result was very promising, further studies using clinical samples (see section *DNA fragments from clinical samples*) showed that incubation at high temperature has a detrimental effect on the probing platform for detection of DNA (see below). Thus, all the remaining experiments were performed at 25 ºC.

At 25 ºC, incubation of the AuNT-noMUT probes for 2 hours does not lead to any significant changes in the LSPR. For an incubation time of 3 hours, a significant LSPR red-shift was observed after hybridization with the complementary target, and an insignificant shift for incubation with the non-complementary target. The results are shown in Table S1 and Figure 4. The best discrimination between complementary and non-complementary targets was observed for AuNT-probes prepared with 1 mM MCH and the more stringent hybridization conditions with 2x SCC. In this case, the shift for hybridization with complementary targets was 34.7 ± 2.6 nm vs. a shift of 1.0 ± 0.5 nm for non-complementary targets. For the less stringent hybridization conditions (5x SSC) a slightly lower LSPR shift was observed, but the differences are not statistically significant.

For AuNTs prepared with 5 mM MCH, the decrease in the LSPR shift upon hybridization is *ca.* 50% for 5x SSC and *ca.* 30% for 2x SSC relative to the shift for AuNTs prepared with 1 mM MCH with 5x SSC and 2x SSC, respectively. This significant decrease in sensitivity can be related to excessive replacement of oligonucleotide by MCH for the higher concentration of MCH used, decreasing the number of oligonucleotides bound to the surface of the nanotriangles, and thus rendering the probes less sensitive to hybridization events.[44] This concentration dependence was not observed for nanospheres. The different behavior between nanospheres and nanotriangles is possibly related to the different curvature of the nanoparticles. The nanotriangles have a flat surface where adsorbed molecules have stronger intermolecular lateral interactions than in curved surfaces (crowding effect).[45] It is expected that stronger lateral contacts will favor the binding of the neutral MCH molecules in comparison with the highly negatively charged thiolated-oligonucleotides, for which strong electrostatic intermolecular repulsions are expected.

It should also be mentioned that the results obtained with the AuNT-probes show a noticeable improvement in terms of sensitivity, in comparison with 80 nm gold nanospheres, for

which a 5 nm-shift upon hybridization with complementary targets was observed.[16] This increased sensitivity can in principle be further improved by using an instrument with detection in the near infrared, since this would allow selecting nanotriangles with resonance peaks at higher wavelengths. The nanotriangles with scattering peaks at higher wavelengths are expected to be more sensitive to changes in the refractive index,[46] but are not suitable for analysis in the present conditions since the plasmon peaks after hybridization are outside the limits of the instrument.

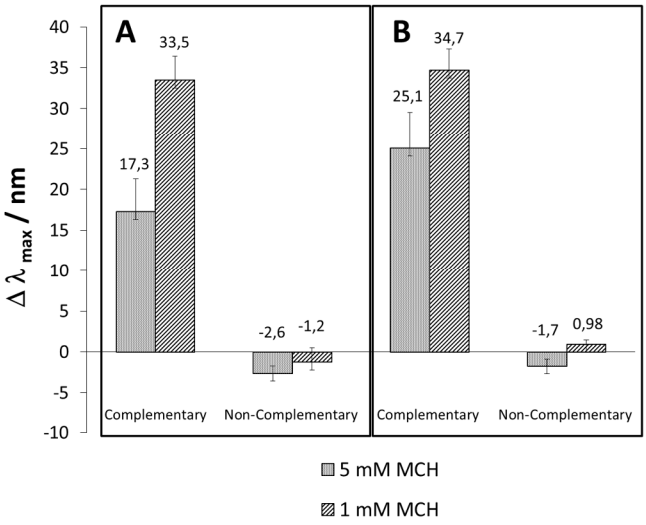

Figure 4: Effect of stringency during the hybridization step; and of MCH concentration during AuNT-probe formation. LSPR shifts ($\Delta\lambda_{max}$) were calculated after hybridization with complementary and non-complementary targets at 25 ºC, for an incubation period of 3 hours. **(A)** 5x SSC; **(B)** 2x SSC. Each bar represents the average signal for 12 AuNT-probes.

DNA fragments from clinical samples

In view of the application of this LSPR based method to clinical samples, the thiolated oligonucleotide noMUT had been designed to specifically hybridize with a 20 bp region situated downstream from position *rs4988235 (13910)* of the gene LCT. This specific hybridization can be used for molecular diagnosis of lactose intolerance.[38] The 20 bp sequence is contained in a PCR fragment of 345 bp. The non-complementary target was a 445 bp PCR fragment amplified from the FTO gene, a region that has total absence of complementarity along the whole fragment (Figure S1).

The experimental conditions for hybridization were the optimized conditions for the system with synthetic targets, with the exception of hybridization temperature. Since the samples are PCR products (dsDNA), the first approach was to perform the experiments at a temperature close to the melting temperature (T_m) of the target fragment on the chip (59 ºC), calculated according to Fotin *et al.*[47] However, under these conditions, extensive movement of the AuNT-probes on the chip was observed, preventing the identification of individual AuNTs after annealing (Figure S4). Possibly the electrostatic interactions, responsible for the AuNT adsorption to the silanized surface are not strong enough, leading to lack of adherence at high temperatures. In addition, the few AuNTs that could be traced back to the original chip position showed LSPR spectra identical to the non-functionalized AuNTs, hinting at desorption of the thiolated oligonucleotide probe.

Considering the fact that the PCR fragment targets could not be denatured *in situ*, a denaturation step was previously performed, to avoid high temperatures on the chip. After 10 minutes at 90 ºC, the PCR fragment sample was placed in an ice-bath to "freeze" the ssDNA. This cooling step allows for the newly formed ssDNA to keep its configuration, allowing its utilization in the hybridization reaction. Although the annealing temperature used for fragments with sizes between 350-450 bp is generally *ca.* 56-62 ºC, hybridization was performed at room temperature, due to the limitations of AuNTs detachment at such elevated temperatures (Figure S4). After hybridization at the experimental conditions previously optimized for the synthetic targets (AuNT-probe synthesis with 1 mM MCH; DNA hybridization for 3 hours, at 25 ºC and 2x SCC) hybridization with the complementary target from the clinical samples yields a large red-shift of 21.6 ± 2.9 nm, whereas no significant shift is observed for the non-complementary target (-0.4 ± 1.1 nm). Such results are in line with the behavior shown by the synthetic targets (Figure 4). These results with PCR fragments from clinical samples, presenting a length that is practically 7 times larger than the synthetic targets, underscores the robustness and practical usefulness of the proposed LSPR-based method in the detection of specific DNA sequences.

Mutation position influence on DNA hybridization

Probe formation with the oligonucleotides with single mutation was carried out regarding the optimized conditions established after the hybridization step for oligonucleotide noMUT, including MCH concentration of 1 mM. According to Figure S3, no significant changes were observed in terms of resonance shift, indicating that the alteration of the oligonucleotide sequence does not compromise the binding of the oligonucleotide and/or any change in the LSPR peak. An average value of around 16 nm for the LSPR shift is observed for all the mutated oligonucleotides.

Hybridization efficiency can be related to single-mutation position along the probe-oligo sequence.[15] Table 2 presents results for hybridization efficiency of AuNT-probes with oligonucleotide presenting mutations in three different positions, namely, at the 5´ terminal, near the thiol and the AuNT (MUT5), in the middle of the sequence (MUT10), and at its 3´terminal (MUT20).

Hybridization of the synthetic target (50 bp) and the AuNT-probe with the mutation at position 5, leads to a resonance shift of 4.1 ± 2.7 nm, indicating a small amount of target binding.

The existence of a mutation near the 5' terminal of the sequence leads to non-complementarity in more than 75% of the probe sequence. In fact, of the 50 bases present in the probe, only four are complementary to the target. Positioning the mutation at the middle, at position 10, leads to a greater percentage of target molecules binding, translated by an average resonance shift of 11.7 ± 4.1. According to the almost double value of the average resonance shift in comparison with the 5' mutation, this result indicates that more targets hybridize, which agrees with a larger complementarity between target and probe. Finally, when the mutation is located at the 3' terminal base there is practically no difference in the resonance shift value, when compared with the fully complementary target (32.4 ± 2.6 nm vs. 34.7 ± 2.4 nm) (Table 2). Thus, the existence of a mismatch in this terminal position does not seem to appreciably affect target hybridization. These results are reinforced by hybridization of the 345 bp PCR product target, a target that is five times longer than the synthetic target. For all mutant three probes tested, the observed resonance shifts are about half of the values obtained for hybridization with the synthetic target (Table 2). This is probably an effect of slower hybridization kinetics due to the low percentage of complementary bases in this 345 bp target.

Table 2 - LSPR shifts ($\Delta\lambda_{max}$) after hybridization of the AuNT-probes with single base mutations in different positions, using either a synthetic or a PCR amplified target, in optimized hybridization conditions. Each result represents the average signal for 12 AuNTs.

Probe oligonucleotide	Synthetic DNA target (50 bp)	PCR product target (345 bp)
MUT5	4.1 ± 2.7	2.0 ± 5.6
MUT10	11.7 ± 4.1	5.4 ± 6.9
MUT20	34.7 ± 2.4	14.2 ± 3.7

Conclusions

A sensing platform containing AuNTs-oligo probes immobilized in a chip was prepared and used as a specific-sequence DNA sensor, based on LSPR spectroscopy and dark field optical microscopy. The sensing platform was evaluated using both synthetic targets and targets obtained from clinical samples. The results obtained show that this platform has an extremely high sensitivity to hybridization events with both types of samples, with LSPR shifts in the order of 35 nm. The high sensitivity of the AuNTs (average side length of 90 nm) to adsorption of molecules was evident even in the preparation of the AuNTs-oligo probes. The shift in the SPR band upon adsorption of the oligonucleotide to the AuNTs was ca. 3 times higher than for spherical nanoparticles of similar size. This behavior has been explained by the existence of "hot spots" on AuNTs, namely on the vertices and on the edges. Additionally the flat surface of nanotriangles can conveniently lead to a more organized packing of the oligonucleotides, and thus a higher number of thiolated oligonucleotides adsorbed per AuNT.[36, 48] We have used synthetic targets to optimize the preparation of the AuNTs probes. In these experiments, we have found that detection is preferably performed at room temperature, in contrast to the usual hybridization conditions used in most methods. In fact, high temperatures promote desorption of both the AuNTs from the chip surface, and the thiolated oligonucleotide probe from the AuNT, hindering further use for detection. Hybridization between the probe adsorbed to the AuNT and the synthetic target is almost complete after 3 hours at room temperature, allowing detection to be performed in these experimental conditions. We have also used 6-mercaptohexanol, to prepare AuNT-probes with a mixed layer of the oligo probe and 6-mercaptohexanol. As previously found for gold nanospheres, this approach improves the sensitivity of the method.[16] However, in the case of the nanotriangles as LSPR sensors, we have found that the concentration of the spacer should be lower 5 times lower than the concentration reported previously for the gold nanospheres.[16] The present findings highlight the importance of optimizing the experimental conditions for the manufacture of the sensing platforms, even in the case of closely related nanoparticles.

The present study has also reinforced the premise that mutation positioning has a direct influence in the hybridization efficacy, indicating that for mutations located close to the surface of the AuNT-probe (near the 5'-end) hybridization efficiency decreases considerably. When mismatch is positioned along the sequence (direction 5' to 3') efficiency starts to increase, *i. e.* a higher number of targets are binding to the AuNT-probe. Conversely, almost no difference in the LSPR shift is observed when the mutation is near the 3' terminal, in comparison with the fully complementary target.

As a proof of concept, we have used DNA targets obtained from clinical samples to assess the possibility of using these platforms in the detection of specific DNA sequences for diagnostics. Results show that, even at room temperature, hybridization with complementary PCR products of 345 bp causes remarkably high LSPR shifts of 22 nm, in comparison to only 3 nm for a similar platform with gold nanospheres.[16] It should also be mentioned that for non-complementary targets LSPR shifts are less than ± 1 nm, showing the high discrimination ability of the present detection platform.

The presented detection system is especially promising for the development of detection methodologies using anisotropic nanoparticles, based on their higher sensitivity; and stimulating the development of DNA biosensors in chips with the possibly of further integration in microfluidics and point-of-care devices.

Acknowledgements

The authors thank Thomas Schneider and Steffen Trautmann for help with LSPR measurements. This work was supported by the European Science Foundation Research Networking Program, "Plasmon-Bionanosense" (exchange grants 3846 and 4136 to visit IPHT by LS); QREN through Project ON2-Nanochemistry; and Fundação para a Ciência e a Tecnologia, and COMPETE Program, Portugal (Grants PEst-C/EQB/LA0006/2013 to LS, EP and RF; PTDC/CTM-NAN/112241/2009 to RF; and PhD grant SFRH/BDE/51100/2010 to LS, a joint venture with STAB-Vida Lda.).

Notes and references

[a] REQUIMTE, Departamento de Química, Faculdade de Ciências e Tecnologia, Universidade Nova de Lisboa , 2829-516 Caparica, Portugal

[b] REQUIMTE, Departamento de Química e Bioquímica, Faculdade de Ciências, Universidade do Porto, 4169-007 Porto, Portugal

[c] STAB-Vida Lda., Madan Parque, 2825-182 Caparica, Portugal

[d] Leibniz Institute of Photonic Technology (IPHT) Jena, 07745 Jena, Germany

* Corresponding author: ricardo.franco@fct.unl.pt

1. K. Saha, S. S. Agasti, C. Kim, X. Li and V. M. Rotello, *Chemical Reviews*, 2012, **112**, 2739-2779.
2. H. Jans and Q. Huo, *Chemical Society Reviews*, 2012, **41**, 2849-2866.
3. G. Doria, J. Conde, B. Veigas, L. Giestas, C. Almeida, M. Assunção, J. Rosa and P. V. Baptista, *Sensors*, 2012, **12**, 1657-1687.
4. P. V. Baptista, G. Doria, P. Quaresma, M. Cavadas, C. S. Neves, I. Gomes, P. Eaton, E. Pereira and R. Franco, in *Progress in Molecular Biology and Translational Science*, ed. V. Antonio, Academic Press, 2011, vol. Volume 104, pp. 427-488.
5. P. Baptista, E. Pereira, P. Eaton, G. Doria, A. Miranda, I. Gomes, P. Quaresma and R. Franco, *Anal Bioanal Chem*, 2008, **391**, 943-950.
6. L. Dykman and N. Khlebtsov, *Chemical Society Reviews*, 2012, **41**, 2256-2282.
7. A. Kumar, B. M. Boruah and X. J. Liang, *Journal of Nanomaterials*, 2011.
8. J. Cortez, E. Vorobieva, D. Gralheira, I. Osório, L. Soares, N. Vale, E. Pereira, P. Gomes and R. Franco, *Journal of Nanoparticle Research*, 2011, **13**, 1101-1113.
9. B. Sepúlveda, P. C. Angelomé, L. M. Lechuga and L. M. Liz-Marzán, *Nano Today*, 2009, **4**, 244-251.
10. C. Maximilien, T. Néné, G. Ana-Maria, L.-G. Nathalie, F. Monica, A. Simion and C. Marc Lamy de la, *Plasmonics*, 2014, **8**, 699-704.
11. A. D. McFarland and R. P. Van Duyne, *Nano Letters*, 2003, **3**, 1057-1062.
12. H. M. Kim, S. M. Jin, S. K. Lee, M.-G. Kim and Y.-B. Shin, *Sensors*, 2009, **9**, 2334-2344.
13. I. Gomes, M. Feio, N. Santos, P. Eaton, A. Serro, B. Saramago, E. Pereira and R. Franco, *Journal of Nanoparticle Research*, 2012, **14**.
14. J. Conde, J. M. de la Fuente and P. V. Baptista, *Journal of Nanobiotechnology*, 2010, **8**, 5.
15. G. Doria, B. G. Baumgartner, R. Franco and P. V. Baptista, *Colloids and Surfaces B: Biointerfaces*, 2010, **77**, 122-124.
16. T. Schneider, N. Jahr, J. Jatschka, A. Csaki, O. Stranik and W. Fritzsche, *Journal of Nanoparticle Research*, 2013, **15**, 1531.
17. J. Fang, L. Yu, P. Gao, Y. Cai and Y. Wei, *Analytical Biochemistry*, 2010, **399**, 262-267.
18. J. N. Anker, W. P. Hall, O. Lyandres, N. C. Shah, J. Zhao and R. P. Van Duyne, *Nat Mater*, 2008, **7**, 442-453.
19. J. E. Millstone, S. J. Hurst, G. S. Métraux, J. I. Cutler and C. A. Mirkin, *Small*, 2009, **5**, 646-664.
20. S. R. Beeram and F. P. Zamborini, *Journal of the American Chemical Society*, 2009, **131**, 11689-11691.
21. T. K. Sau, A. L. Rogach, F. Jäckel, T. A. Klar and J. Feldmann, *Advanced Materials*, 2010, **22**, 1805-1825.
22. A. J. Haes, S. Zou, G. C. Schatz and R. P. Van Duyne, *The Journal of Physical Chemistry B*, 2004, **108**, 6961-6968.
23. S. K. Kim, H. Cho, J. Jeong, J. N. Kwon, Y. Jung and B. H. Chung, *Chemical Communications*, 2010, **46**, 3315-3317.
24. C. Sonnichsen, B. M. Reinhard, J. Liphardt and A. P. Alivisatos, *Nat Biotech*, 2005, **23**, 741-745.
25. W. P. Hall, S. N. Ngatia and R. P. Van Duyne, *J Phys Chem C Nanomater Interfaces*, 2011, **115**, 1410-1414.
26. R. Q. Duan, J. L. Yuan, H. Yang, X. G. Luo and M. R. Xi, *Neoplasma*, 2012, **59**, 348-353.
27. P. C. Linic, X. Hongliang and Suljo, *Nature Chemistry*, 2011, **3**, 467-472.
28. D. Aherne, D. E. Charles, M. E. Brennan-Fournet, J. M. Kelly and Y. K. Gun'ko, *Langmuir*, 2009, **25**, 10165-10173.
29. P. Baptista, G. Doria, D. Henriques, E. Pereira and R. Franco, *Journal of Biotechnology*, 2005, **119**, 111-117.
30. P. Eaton, G. Doria, E. Pereira, P. V. Baptista and R. Franco, *IEEE Trans Nanobioscience*, 2007, **6**, 282-288.
31. G. Doria, R. Franco and P. Baptista, *IET Nanobiotechnology*, 2007, **1**, 53-57.
32. C. A. Mirkin, R. L. Letsinger, R. C. Mucic and J. J. Storhoff, *Nature*, 1996, **382**, 607-609.
33. A. B. Steel, T. M. Herne and M. J. Tarlov, *Analytical Chemistry*, 1998, **70**, 4670-4677.
34. A. Miranda, E. Malheiro, E. Skiba, P. Quaresma, P. A. Carvalho, P. Eaton, B. de Castro, J. A. Shelnutt and E. Pereira, *Nanoscale*, 2010, **2**, 2209-2216.
35. Y. Fang and J. H. Hoh, *Nucleic Acids Research*, 1998, **26**, 588-593.
36. T. M. Herne and M. J. Tarlov, *Journal of the American Chemical Society*, 1997, **119**, 8916-8920.
37. R. Levicky, T. M. Herne, M. J. Tarlov and S. K. Satija, *Journal of the American Chemical Society*, 1998, **120**, 9787-9792.
38. N. S. Enattah, T. Sahi, E. Savilahti, J. D. Terwilliger, L. Peltonen and I. Jarvela, *Nat Genet*, 2002, **30**, 233-237.
39. S. F. Altschul, W. Gish, W. Miller, E. W. Meyers and D. J. Lipman, *Journal of Molecular Biology*, 1990, **215**, 403-410.
40. C. Yu and J. Irudayaraj, *Biophys J*, 2007, **93**, 3684-3692.
41. N. Cottenye, F. Teixeira, A. Ponche, G. Reiter, K. Anselme, W. Meier, L. Ploux and C. Vebert-Nardin, *Macromolecular Bioscience*, 2008, **8**, 1161-1172.
42. A. B. Steel, R. L. Levicky, T. M. Herne and M. J. Tarlov, *Biophys J*, 2000, **79**, 975-981.
43. R. Levicky, T. M. Herne, M. J. Tarlov and S. K. Satija, *Journal of the American Chemical Society*, 1998, **120**, 9787-9792.
44. C. Cotton, A. Glidle, G. Beamson and J. M. Cooper, *Langmuir*, 1998, **14**, 5139-5146.
45. R. Franco and E. Pereira, in *Encyclopedia of Metalloproteins.*, ed. R. H. U. Kretsinger, V.N.; Permyakov, E.A. , Springer Science+Business Media New York, 2013, pp. 908-915.
46. M. M. Miller and A. A. Lazarides, *The Journal of Physical Chemistry B*, 2005, **109**, 21556-21565.
47. A. V. Fotin, A. L. Drobyshev, D. Y. Proudnikov, A. N. Perov and A. D. Mirzabekov, *Nucleic Acids Research*, 1998, **26**, 1515-1521.
48. A. Csaki, R. Moller, W. Straube, J. M. Kohler and W. Fritzsche, *Nucleic Acids Res*, 2001, **29**, e81.

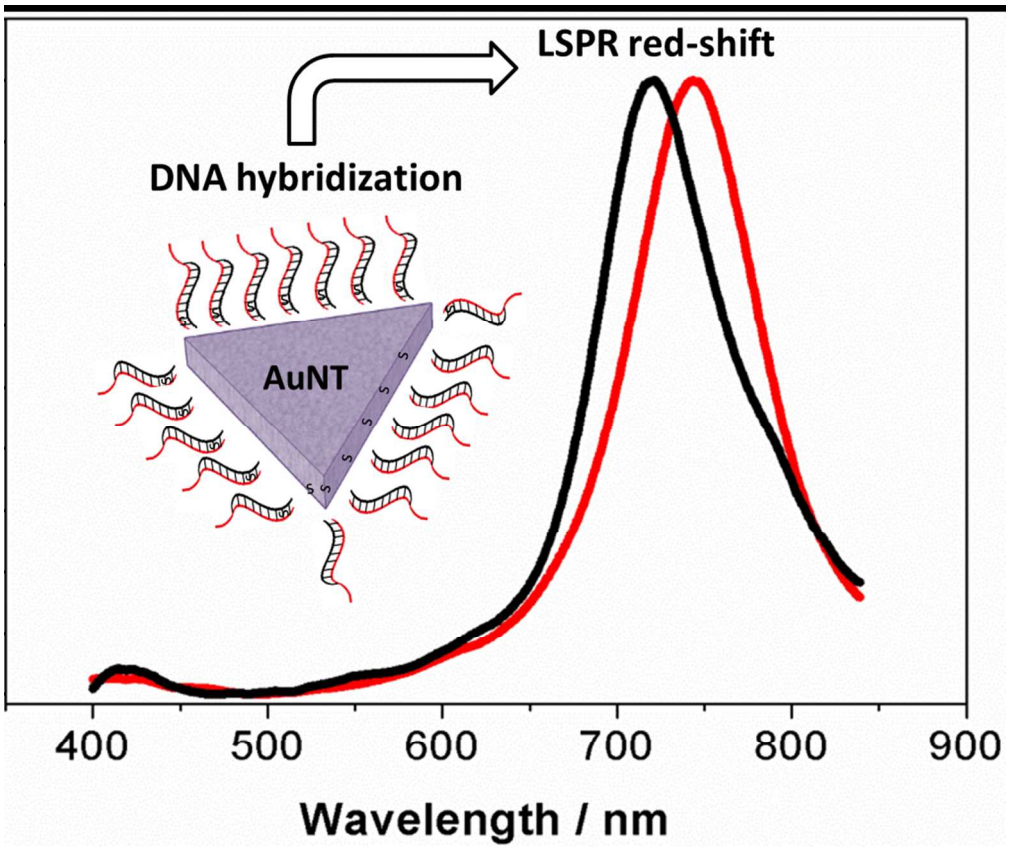

Hybridization of target DNA to AuNT-probes causes LSPR to red-shift
171x144mm (150 x 150 DPI)